Investigation on the Electronic and Optical Properties of Short Oxidized Multiwalled Carbon Nanotubes

ARTICLE *in* THE JOURNAL OF PHYSICAL CHEMISTRY C · JULY 2010

Impact Factor: 4.77 · DOI: 10.1021/jp101868s

8 AUTHORS, INCLUDING:

Simona Torrengo
Atomic Energy and Alternative Energies Co…
22 PUBLICATIONS **165** CITATIONS
SEE PROFILE

Barbara Rossi
Elettra, Sincrotrone Trieste S.C.p.A.
63 PUBLICATIONS **429** CITATIONS
SEE PROFILE

Maurizio Ferrari
Italian National Research Council
520 PUBLICATIONS **5,464** CITATIONS
SEE PROFILE

Alessandro Chiasera
Italian National Research Council
237 PUBLICATIONS **2,222** CITATIONS
SEE PROFILE

Investigation on the Electronic and Optical Properties of Short Oxidized Multiwalled Carbon Nanotubes

L. Minati,*,† G. Speranza,† I. Bernagozzi,† S. Torrengo,†,‡ L. Toniutti,‡ B. Rossi,‡ M. Ferrari,§ and A. Chiasera§

FBK, Via Sommarive 18, Povo 38123 Trento, Italy, Department of Physics, University of Trento, Via Sommarive 14, Povo 38123 Trento, Italy, and CNR-IFN, CSMFO Lab. Via alla Cascata, 56/C, Povo 38123 Trento, Italy

Received: March 2, 2010; Revised Manuscript Received: May 13, 2010

Oxidized multiwalled carbon nanotubes were produced by strong acid treatment with the aid of sonication. Short-length carbon nanotubes obtained by filtration of the oxidized carbon nanotubes were analyzed by means of X-ray photoelectron spectroscopy, Raman and photoluminescence spectroscopies, and scanning electron microscopy. Direct evidence of the modifications of the electronic properties of the carbon nanotubes was obtained by the valence band analysis. The oxidation induced by the acid treatment led to deep changes of the carbon nanotubes density of states. Analysis of the photoluminescence spectra showed that the short carbon nanotubes are luminescent in the visible range. Interestingly, the spectral intensities and lineshapes are strongly dependent on the pH of the CNT solution. This effect is explained by a modification of the local environment of the defects induced by the protonation/deprotonation of the carboxylic groups formed by the oxidation process.

Introduction

In recent years the photoluminescence properties of carbon nanotubes (CNTs) have generated a great interest in potential applications of these 1D nanosystems in nanoelectronics, photonics, and sensoristics and have triggered the attention of the research community toward the study of the process underlying their exceptional physical properties.[1–3] Moreover, the possibility of functionalize carbon nanotubes with covalent bonding of appropriated functional groups makes both the carbon nanotubes handling and production of carbon nanotubes tailored for specific applications easier.[4–7] One of the most important and recent advances in this area concerns the photoluminescence properties of nanotubes, which can introduce these nanostructures in the field of photonics. In particular, the single-walled carbon nanotubes have a near-infrared luminescence (900−1300 nm). This luminescence was shown to originate from electronic transitions between the Van Hove singularities[8] induced by the absorption of photons. Generally, this type of luminescence being very weak is useful only to recognize the different nanotubes chiral species. Only very recently was Ju,[9] using a method of oxygen exclusion obtained with a proper surfactant, able to obtain an optical efficiency of around 20%.

The discovery of the visible luminescence of the carbon nanotubes in solution by Riggs[10] has opened the way to the investigation of the electronic properties of functionalized carbon nanotubes. The visible luminescence represents an interesting property of the carbon nanotubes. This was confirmed by several studies presented in the literature.[11,12] The mechanism nowadays is still the object of controversy, but the defect states introduced by the functionalization seem to be the principal reason for the visible luminescence.[10] These defects are introduced in the carbon nanotubes backbone by an oxidation treatment, generally by strong oxidizing agents as nitric acid or sulfuric−nitric acid mixtures.[14] The introduction of a certain number of defects leads to a remarkable change of the electronic structure near the Fermi level,[13] which can explain the optical properties of the nanotubes.

It is interesting to note that both single-wall and multiwall carbon nanotubes present similar optical properties after oxidation. Moreover, also other carbon nanostructures such as carbon nanoparticles show luminescence in the visible regions when treated with strong oxidizing agents.[15] The formation of carbon−oxygens bonds, such as in oxidrilic and carboxylic groups, seems to be a *contitio sine qua non* for the production of luminescent carbon-based materials. The formation of carboxyl groups can also be exploited to anchor functional molecules or polymer chains via amidation or esterification reactions. The passivation of the defects by appropriated functional groups leads to an increase of the luminescence of the carbon nanotubes and improves the dispersion of the CNT in the solution, limiting the nonradiative decay path.[11] The aim of this paper is to study the oxidation process accomplished by a nitric−sulfuric acid mixture in order to obtain information about the modifications in the carbon nanotubes electronic properties. The characterization was performed by using several techniques such as X-ray photoelectron spectroscopy (XPS), Raman and photoluminescence (PL) spectroscopies, and scanning electron microscopy (SEM). The oxidized-short carbon nanotubes show also an interesting dependence of the photoluminescence shape and intensity on the pH of the solution indicating that the defect surrounding media plays an important role in the luminescence mechanism.

Experimental Section

Pristine multiwalled carbon nanotubes (p-CNT) (Nanoamor USA) were cut by acid in a (1:3) HNO_3/H_2SO_4 mixture,

* To whom correspondence should be addressed.
† FBK.
‡ University of Trento.
§ CNR-IFN.

10.1021/jp101868s
Published on Web 06/04/2010

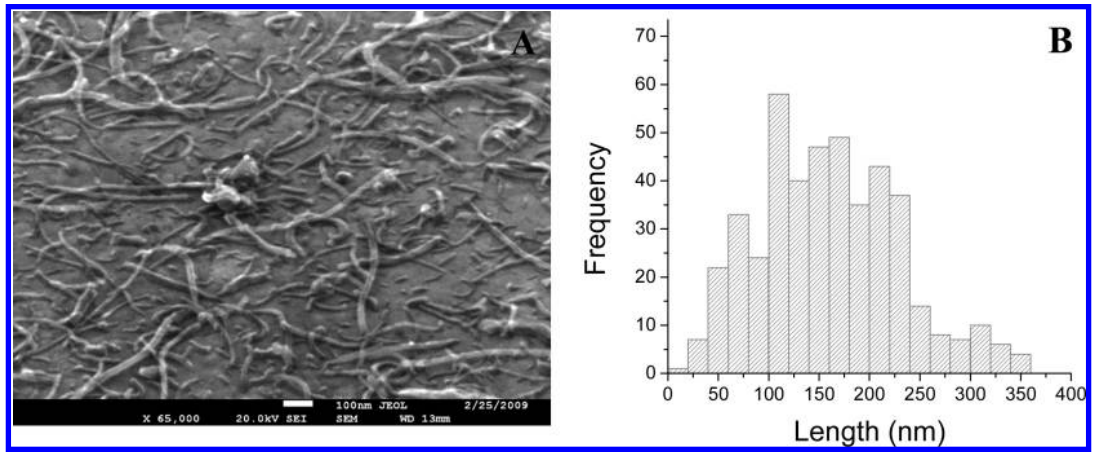

Figure 1. (A) Scanning electron microscopy image of the acid treated carbon nanotubes deposited on gold substrate obtained with a 45° tilt. (B) Histogram of the length distribution calculated by analyzing different SEM images.

followed by ultrasonication for 12 h at 40 °C. The black suspension was then diluted with water and allowed to stand overnight for precipitation.

After the removal of the supernatant, the suspension was diluted with deionized water and filtered with a 0.05 μm filter membrane under vacuum. The precipitate was successively washed with a 0.1 M NaOH water solution to eliminate carbon fragments or oxidation debris that could be produced by the acid treatment and then rinsed with 0.1 M HCl water solution until neutrality of the filtrate.[16] The oxidized carbon nanotubes (o-CNT) obtained were found to form stable colloidal suspensions in plenty of solvents including water, ethanol, and dimethylformamide. The oxidized carbon nanotubes solution was further filtrated under vacuum onto a 0.2 μm PTFE membrane to separate the short carbon nanotubes (so-CNT). Some drops of solution of the short CNTs were spread on a gold substrate and then analyzed with scanning electron microscopy for the length distribution analysis.

The short carbon nanotubes were successively spread on silica-coated silicon substrate until the formation of a thick carbon nanotube film. These films were then characterized by X-ray photoelectron spectroscopy and Raman spectroscopy. Finally, the short carbon nanotubes dissolved in solution at different pH values obtained by addiction of controlled amounts of HCl or NaOH were analyzed by visible absorption spectroscopy and photoluminescence spectroscopy.

The XPS measurements were carried out with an ESCA200 instrument (Scienta-Gammadata ESCA 200 Uppsala Sweden). Wide scans were acquired in the BE energy range 1200−0 eV with a 500 eV pass energy while high-resolution core line spectra were performed setting the analyzer pass energy at 150 eV and the energy step at 0.05 eV. The valence band regions were acquired by setting 300 eV pass energy with an energy step of 0.1 eV. Because the samples are conductive, they do not require charge compensation, leading to an energy resolution of 0.3 eV measured on the Ag Fermi edge. Scanning electron microscopy analysis was carried out in a JSM-7001F instrument equipped with a thermal field emission gun. Images were acquired with samples placed at 45° with respect to the analyzer direction.

Raman scattering measurements were performed in a wide wavenumber range between 300 and 5000 cm^{-1} by means of a microprobe setup (Horiba-Jobin-Yvon, model Labram HR) consisting of a He−Ne laser operating at 633 nm (power 15 mW), a narrow-band notch filter, an 80-cm focal length spectrograph, a 600 grooves/mm grating, as well as a charge-coupled device (CCD) detector with red-extended response that was cryogenically cooled by liquid nitrogen. The laser beam was focused onto the sample surface with a spot size of about 2 μm by using a 100 objective with NA = 0.9. To avoid unwanted laser-induced transformations, neutral filters of different optical densities were used whenever necessary. In this configuration the resolution was about 1 cm^{-1}/pixel.

UV−vis absorption measurements were performed with an UV−visible−near-infrared spectrophotometer (Cary 5000) in dual beam mode. Photoluminescence (PL) measurements in the 400−800 nm regions were obtained upon excitation with the 514.5 and 456.3 nm lines of an Ar^+ ion laser.

Results and Discussions

The scanning electron microscopy analysis of the o-CNT sample is reported in Figure 1A. The initial lengths of the carbon nanotubes were between 0.5 and 2 μm. After the acid treatment the length distribution is in the range 0−1 μm with a mean value of around 300−400 nm. In Figure 1B, the calculated length distribution is reported. As expected, the acid treatment leads to a decrease of the mean length of the carbon nanotubes and a considerable fraction of carbon nanotubes with length lower than 200 nm are present. These small carbon nanotubes are expected to present a higher density of functional groups and a higher luminescence as previously reported in the literature.[17] To put in evidence the presence of these short carbon nanotubes the sample was filtered with a 0.2 μm pore filter. The yellow-brown filtrate obtained was then spread onto gold substrate and analyzed with scanning electron microscopy.

The SEM image reported in Figure 2 shows that the carbon nanotubes filtrate contains small carbon nanotubes (mean length around 100−150 nm) as well as ultrashort CNTs ($L < 100$ nm). This confirms that the acid treatment is very effective in attacking the CNTs and producing shorter systems provided with oxygen-containing functional groups.

The XPS analyses were performed after the deposition of a thick film of the o-CNT and so-CNT on a silica/silicon substrate. In Figure 3A, C1s of the pristine, oxidized, and short carbon nanotubes and fit of the so-CNT C1s (B) are reported. No evidence of other elements besides carbon and oxygen is revealed by the XPS analysis. It appears evident that the oxidized sample C1s spectra are substantially different with respect to that of the pristine carbon nanotubes. In particular, the region between 290 and 285 eV reveals the presence of a high number of carbon−oxygen bonds. In Table 1 are reported the quanti-

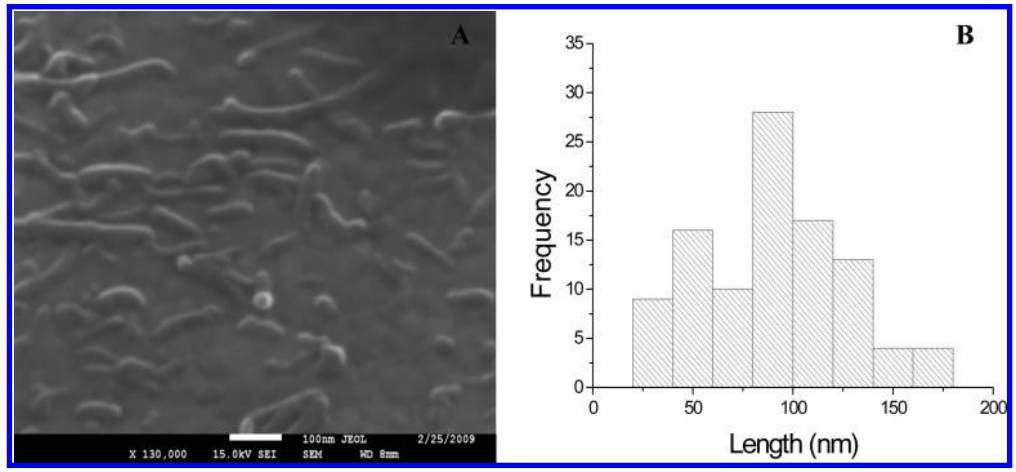

Figure 2. (A) Scanning electron microscopy image of the so-CNT sample deposited on gold substrate. (B) Histogram of the length distribution calculated by analyzing different SEM images.

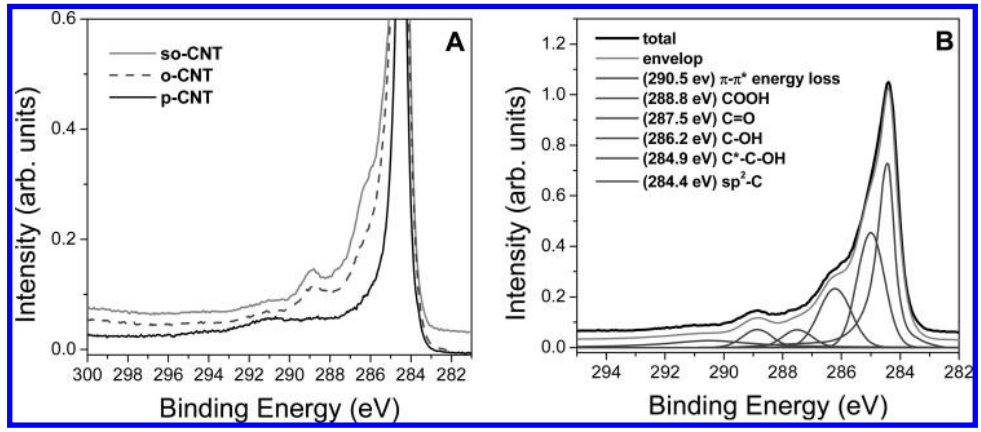

Figure 3. (A) Overlay of the XPS C1s core lines of the p-CNT, o-CNT, and so-CNT samples. The spectra are vertically shifted for clarity. (B) Peak fitting of the C1s region of so-CNT sample obtained by using Voight line shape for the sp^2 component and Gaussian for the other peaks and Shirley background subtraction.

TABLE 1: XPS Binding Energies, Atomic Abundances, and Chemical Bonds[a]

component	BE (eV)	p-CNT concn (at %)	o-CNT concn (at %)	so-CNT concn (at %)	bond
C1s1	288.81		2.30	3.49	COOH
C1s2	287.49		2.05	3.71	C═O
C1s3	286.19	3.32	9.83	13.98	C−OH, C−O−C
C1s4	284.95	3.74	23.06	27.28	C*−C−O
C1s5	284.40	89.43	48.05	31.47	sp^2C
O1s1	533.55		2.25	3.73	COO*H
O1s2	532.50	3.51	10.31	13.06	C−OH, C−O−C, C═O
O1s3	531.78		2.15	3.28	CO*OH

[a] Assignments were made on the basis of the peak fitting of the C1s and O1s core lines analysis relative to the p-CNT, o-CNT, and so-CNT samples.

fication results and the bond assignments relative to the three samples displayed in Figure 3A. In oxidized carbon nanotubes the C1s core line presents a high number of carbon oxygens bonds, like carboxyl (288.81 eV), carbonyl (287.49 eV), and hydroxyl and ether-like bonds (286.19 eV), as well as vicinal carbon atoms (284.95 eV) and sp^2 carbon atoms from the carbon nanotubes backbone (284.40 eV) (see NIST X-ray Photoelectron Spectroscopy Database http://srdata.nist.gov/xps/for the assignment of the chemical bonds).

The XPS quantitative analysis on the three samples reveals that the pristine carbon nanotubes contain a small amount of oxygen (<4 at %) probably coming from the purification procedure. As expected the shorter carbon nanotubes possess a higher amount of oxygen (20.5 at %) with respect to the long oxidized carbon nanotubes (14.7 at %). This is because the acid etching of the carbon backbone causes the formations of a number of defects and functional groups placed mainly on the CNT tips. In particular, in so-CNT an oxygen concentration of 18.5% corresponds to a fraction of oxidized carbon atoms equal to ∼28% of the total carbon atoms. Such a large number of oxygen atoms drastically modifies the electronic configurations of the carbon nanotubes.

The presence of a high concentration of defects in the short carbon nanotubes is confirmed by the Raman spectroscopy analysis of the so-CNT sample reported in Figure 4. In the range between 900 and 1900 cm^{-1}, the spectra of o-CNT and so-CNT samples exhibit some Raman peaks assigned to D mode (1330 cm^{-1}), G mode (1582 cm^{-1}), and D′ mode (1608 cm^{-1}). The G-band represents the in-plane tangential stretching of the carbon−carbon bonds. The D and D′ modes reflect the presence of structural disorder on the graphite plane of the nanotubes.[18] Corrosion effects and extended imperfections of the pristine "graphitic-like" structure induced by acid treatment can be clearly observed by the changes of vibrational responses of the morphology of the MWCNTs. For instance, the D mode in the oxidized and short carbon nanotubes is significantly enhanced as compared to that of the pristine carbon nanotubes. In the o-CNT and so-CNT samples, the intensity ratio (D/G) is around

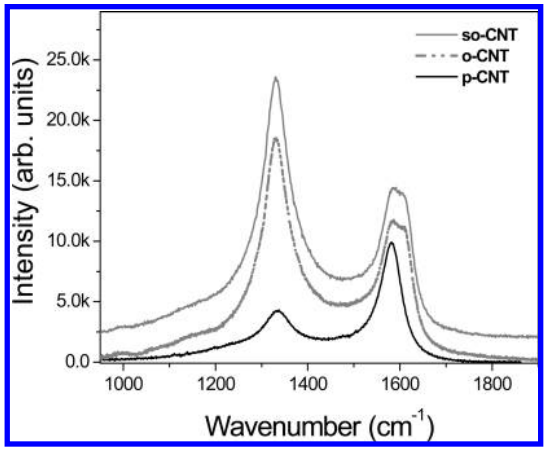

Figure 4. Raman spectroscopy analysis of the p-CNT, o-CNT, and so-CNT samples in the 900−1900 cm^{-1} region acquired with 633 nm excitation wavelength. Spectra are vertically shifted for clarity. The increase of the D component at around 1330 cm^{-1} is evident in the o-CNT and so-CNT induced by the presence of defects.

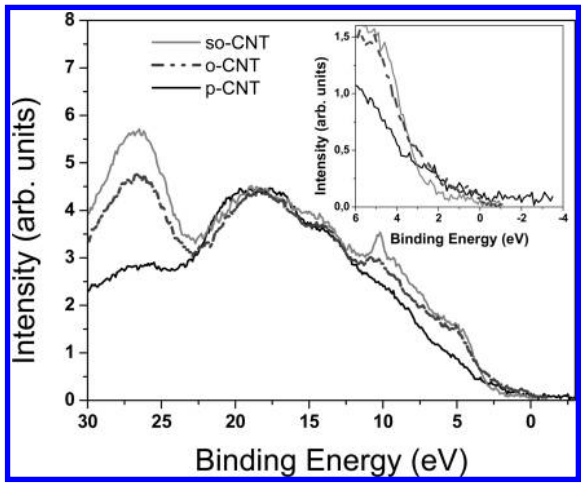

Figure 5. X-ray photoelectron spectra of valence band regions of the pristine, oxidized, and short carbon nanotubes. The peak at around 27 eV is associated to the O2s component. Insert: Regions near the Fermi level for the three samples at higher magnification.

1.55 and 1.62, respectively, while for p-CNT sample the value is 0.42. The higher D/G ratio in o-CNT and so-CNT with respect to that in p-CNT correlates well with a higher defect density leading to an increase of disorder in the CNT structure.

Finally, in Figure 5 the XPS valence band regions (VB) of the pristine, oxidized, and short carbon nanotubes are reported.

The VB deriving from the three CNT samples show marked differences between them. The p-CNT valence band appears very similar to that of pyrolitic graphite. Only a small contribution of oxygen is visible mainly at ∼26 eV and is due to the O2s feature. The spectra of the other two samples appear more structured, which is an indication of the modifications of the electronic structure of the CNT.

The o-CNT and so-CNT spectra show a well-defined peak at around 11 eV. This was already described by other works in the literature and it is assigned to the σ_p contribution deriving from the presence of C−O bonds induced by the acid treatment.[19] The spectra display also marked differences in the region near the Fermi level where there is a progressive loss of density of states in the region 2−0 eV with an increase in the number of oxidized carbon atoms. This is in agreement with results obtained by other authors from the valence band analysis of oxidized and functionalized carbon nanotubes.[20] The decrease of the spectral intensity near the Fermi level leads to the appearance of a band gap. This is reasonable because the oxidation treatment is known to destroy the CNT crystalline structure, with a decrease of the π contribution located in the 2−0 eV region. On the contrary, theoretical calculations show that the formation of defects or functional groups on the surface of the CNTs should lead to an *increase* of the DOS near the Fermi level.[21] This arises from the formation of singular orbitals induced by the presence of the functional groups and defects. For example, Suzuki et al.[22] studied the photoemission spectra obtained from aligned carbon nanotubes by using a scanning photoelectron microscope. Those authors observed an increase of the photoemission signal in the region 2−0 eV from the tip of the nanotubes with respect to the sidewall. They attributed this effect to a higher concentration of structural defects placed on the tip of the nanotubes. Density functional calculations of carboxyl-containing carbon nanotubes[21] show that carboxyl groups and heptagon defects bands contributions fall respectively at −1.6 and −0.1 eV in the valence band region. As can be seen from the C1s analysis of the so-CNT sample, a large number of functional groups (primarily oxidrilic groups) are present in this sample. This leads to the formation of a large number of heptagon and/or pentagon rings. In addition, in a previous paper we showed that the valence band spectrum of 40 min Ar^+ sputtered graphite displayed an increase of signal in the region near the Fermi energy with respect to that of the pristine high oriented pyrolitic graphite.[23] The presence of these states near the Fermi level *does not* induce an increase of the conductive properties of the carbon nanotubes. In both experiments, these states arise from the formation of singular molecular orbitals due to the oxidation process and to the formation of defects and dangling bonds as in the case of ion irradiation. Electron charge confined in these orbitals is strongly localized, a situation markedly different from that of the delocalized nearly free π-electrons responsible of the semimetallic character of multiwall CNT.

The presence of defects-state near the Fermi level in the so-CNT sample was confirmed also by the photoluminescence spectroscopy analysis. Defective and oxidized carbon nanotubes are well-known to be photoluminescent in the visible region.[17] It is generally accepted that the luminescence is a consequence of the ability of defects to trap excitons which can relax with photon emission. It is important to note that not only the intensity but also the emission wavelength of this luminescence are dependent on the excitation energy (normally the maximum of intensity is obtained with a near-UV excitation). A change of the excitation energy leads to a change of the maximum emission wavelength as well as a change of the emission line shape. In our opinion the reason for this behavior stems from the presence of nonequivalent emission sites due to the dispersion of the defect energy. In Figure 6A the photoluminescence spectra of the so-CNT acquired at two different excitation energies are reported. As expected, the luminescence of the carbon nanotubes displays a higher intensity when irradiated with 456.3 nm light. In Figure 6B the UV−vis absorption spectrum of the so-CNT sample is shown. This line shape is the typical fingerprint of the carbon nanotubes with a wide band at around 200−400 nm due to the π plasmon absorption.[24]

Figure 7 displays PL spectra of water solutions of so-CNT acquired at different pH values. It is interesting to observe that the intensity of the yellow component at 560 nm decreases by increasing the pH of the solution. As a matter of fact, the luminescence of the short carbon nanotubes goes from the

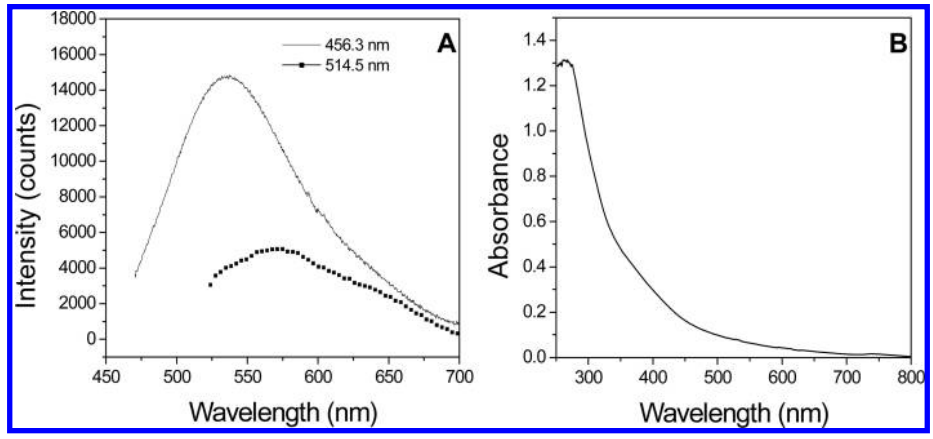

Figure 6. (A) Photoluminescence spectra of the so-CNT sample at two different wavelength excitations (456.3 and 514.5 nm). (B) UV−vis absorption spectra of so-CNT sample in ethanol solution.

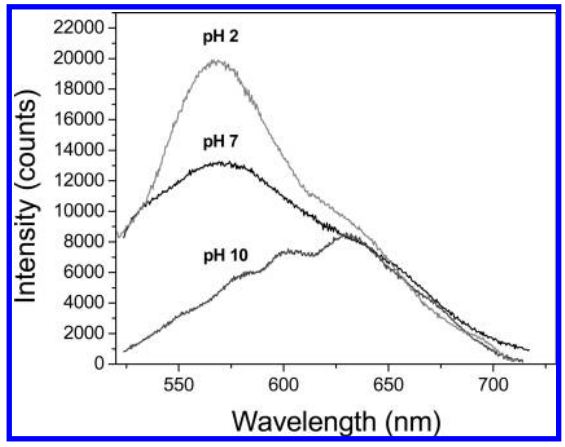

Figure 7. Change of the intensity of the photoluminescence spectra of the so-CNT sample obtained with an excitation wavelength of 514.5 nm and setting the CNT suspension pH at values 2, 7, and 10.

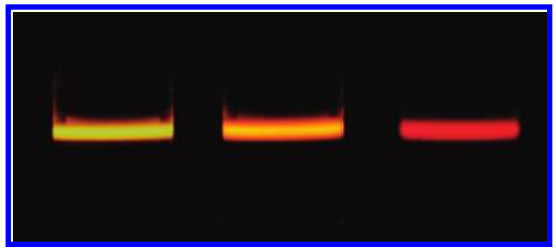

Figure 8. Photographs of the luminescence of the so-CNT sample at pH 2 (left), 7 (center), and 10 (right). The photographs were obtained with a laser excitation of 514.5 nm with a Sapphire filter placed in front of the camera objective.

yellow at pH 2 to the yellow-orange at pH 7 to the red at pH 10 as illustrated in Figure 8. It is reasonable to attribute this effect to the deprotonation of the carboxylic groups, because this is the only functional group sensitive to the pH of the solution. In fact, from the literature, the pK_a of the benzoic acid-modified graphite (a good model of the oxidized carbon nanotubes) was estimated to be around 6.45.[27] The other functional groups like oxidril and carbonyl having a pK_a > 10 cannot interact with the H^+ or OH^- ions of solutions with pH in the range 2−10. Therefore, an increase in the pH value determines a deprotonation of the carboxylic groups with a quenching of the relative emission, while leaving C═O and C−OH sites at ∼635 nm unaffected. As a result, the intensity of the component at 560 nm drastically decreases when the pH of the solution is increased to a value above 7. The fraction *f* of deprotonated carboxylic groups can be retrieved accordingly

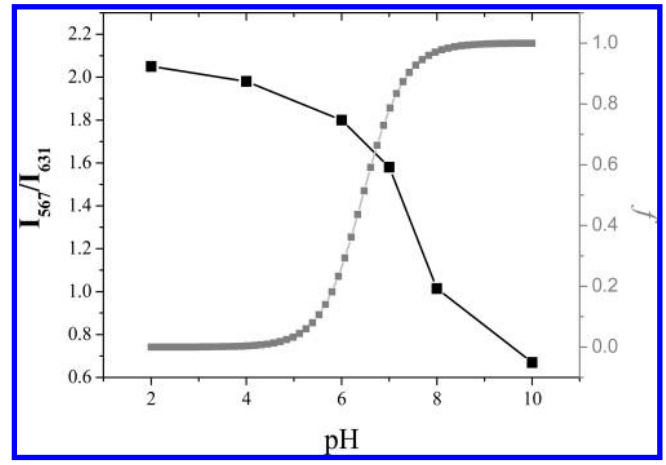

Figure 9. Trend of the spectral intensities ratio measured at 567 and 631 nm (left axes) and the calculated fraction of the deprotonated carboxylic groups (right axes) as functions of the CNT suspension pH.

to the following equation: pH = pK_a + log([CNT−COO^-]/[CNT−COOH]). At pH above 7 in the carbon nanotubes *f* is expected to be higher than 70%.

Figure 9 shows the ratio of the intensities at 567 and 631 nm for different pH values (left axes). For comparison, also the trend of *f* is reported. Interestingly the trend of the ratio of the PL intensity has an opposite trend with respect to that of *f* supporting our hypothesis. Then with a change of the pH we can modulate the strength of the interaction between polar groups, such as the carboxyl group, and the environment. A more detailed investigation is needed to exactly explain the emission changes to the perturbations of specific electronic levels of the functionalized CNT. We observe that PL from functionalized CNTs described here has a different behavior with respect to other carbon-based organic materials. In the case of polycyclic aromatic compounds, (PAH) with acid functional groups, like fluorescein or other pyrene-derived molecules, the luminescence intensity increases with the increase of the pH of the solution. In this case, the light intensification derives from an increased electron transfer from the COOH groups to the xanthene rings in alkaline conditions.[26]

On the other hand, also another kind of inorganic carbon-based nanosystem shows pH dependences of their PL. For example, oxidized carbon nanoparticles obtained from electro-oxidation of graphite present a maximum of luminescence at pH ∼4.5 and a decrease of the luminescence intensity for both higher and lower pH value.[27] Differently, for oxidized carbon

nanoparticles obtained from nitric acid oxidation of candle soot, the maximum of the fluorescence intensity falls at neutral pH and, as previously, decreases significantly upon changing from a neutral to either an acid or a basic pH.[28] Finally, for hydrothermally cut graphene, the luminescence maximum is obtained at pH 13, while the luminescence decreases drastically in acid conditions.[29]

All these examples show different behaviors with respect to that of the short carbon nanotubes. Here we propose that the mechanism underlying the PL behavior of the so-CNT sample is correlated to the changes of the local environment near the COOH groups that lead to modifications of the luminescence behavior of the carbon nanotubes.

Conclusions

In conclusion, short-oxidized carbon nanotubes produced by acid treatment under sonification were characterized by different microscopy and spectroscopic techniques. The analyses put in evidence the presence of a large number of oxygen-containing functional groups such as oxidrilic, carbonylic, and carboxylic. The short carbon nanotubes (with length lower than 200 nm) show a high luminescence in the visible region and a pH sensitivity of the photoluminescence line shape. The PL behavior of this system does not present an analogue among the other carbon-based luminescent nanostructures as carbon dots or graphene oxide. The modification of the shape and position of the PL line in short carbon nanotubes is explained with the modification of the local environment near charged defects (carboxylic groups). In particular the partial suppression of the emission at ~560 nm was associated to a deprotonation of the carboxylic groups.

Acknowledgment. This research was performed in the framework of the COST Action MP0702, and Nanosmart research projects.

References and Notes

(1) Dresselhaus, M. S. *Synthesis, Structure, Properties, and Applications*; Springer.
(2) Odom, T. W.; Huang, J.-L.; Kim, P.; Lieber, C. M. *Nature* **1998**, *391*, 62.
(3) Collins, P. G.; Bradley, K.; Ishigami, M.; Zettl, A. *Science* **2000**, *287*, 1801.
(4) Borghetti, J.; Derycke, V.; Lenfant, S.; Chenevier, P.; Filoramo, A.; Goffman, M. *Adv. Mater.* **2006**, *18*, 2535.
(5) Guo, Z.; Du, F.; Ren, D. M.; Chen, Y. S.; Zheng, J. Y.; Liu, Z. B.; Tian, J. *J Mater Chem* **2006**, *16*, 3021.
(6) Zhang, Y.-B.; Kanungo, M.; Ho, A. J.; Freimuth, P.; van der Lelie, D.; Chen, M.; Khamis, S. M.; Datta, S. S.; Johnson, A. T. C.; Misewich, J. A.; Wong, S. S. *Nano Lett* **2007**, *7*, 3086.
(7) Robel, I.; Bunker, B. A.; Kamat, P. V. *Adv. Mater.* **2005**, *17*, 2458.
(8) Bachilo, S. M.; Strano, M. S.; Kittrell, C.; Hauge, R. H.; Smalley, R. E.; Weisman, R. B. *Science* **2002**, *298*, 2361.
(9) Ju, S.-Y.; Kopcha, W. P.; Papadimitrakopoulos, F. *Science* **2009**, *323*, 1319.
(10) Riggs, J. E.; Guo, Z.; Carroll, D. L.; Sun, Y. P. *J. Am. Chem. Soc.* **2000**, *122*, 5879.
(11) Lin, Y.; Zhou, B.; Martin, R. B.; Henbest, K. B.; Harruff, B. A.; Riggs, J. E.; Guo, Z.-X.; Allard, L. F.; Sun, Y.-P. *J. Phys. Chem. B* **2005**, *109*, 14779.
(12) Sun, Y.-P.; Zhou, B.; Henbest, K.; Fu, K.; Huang, W.; Li, Y.; Taylor, S.; Carroll, D. L. *Chem. Phys. Lett.* **2002**, *351*, 349.
(13) Lim, S. C.; Jo, C. S.; Jeong, H. J.; Shin, Y. M.; Lee, Y. H.; Samayoa, I. A.; Choi, J. *Jpn. J. Appl. Phys.* **2002**, *41*, 5635.
(14) Rosca, I. D.; Watari, F.; Uo, M.; Akasaka, T. *Carbon* **2005**, *43*, 3124.
(15) Sun, Y.-P.; Zhou, B.; Lin, Y.; Wang, W.; Fernando, K. A. S.; Pathak, P.; Meziani, M. J.; Harruff, B. A.; Wang, X.; Wang, H.; Luo, P. G.; Yang, H.; Kose, M. E.; Chen, B.; Veca, L. M.; Xie, S.-Y. *J. Am. Chem. Soc.* **2006**, *128*, 7756.
(16) Verdejo, R.; Lamoriniere, S.; Cottam, B.; Bismarck, A.; Shaffer, M. *Chem. Commun.* **2007**, *5*, 513.
(17) Luo, Y.; Xia, X.; Liang, Y.; Zhang, Y.; Ren, Q.; Li, J.; Jia, Z.; Tang, Y. *J. Solid State Chem.* **2007**, *180*, 1928.
(18) Hiura, H.; Ebbesen, T. W.; Tanigaki, K. *Chem. Phys. Lett.* **1993**, *202*, 509.
(19) Shiraishi, M.; Swaraj, S.; Takenobu, T.; Iwasa, Y.; Ata, M.; Unger, W. E. S. *Phys. Rev. B* **2005**, *71*, 125419.
(20) Bergeret, C.; Cousseau, J.; Fernandez, V.; Mevellec, J.-Y.; Lefrant, S. *J. Phys Chem C* **2008**, *112*, 16411.
(21) Wang, C.; Zhou, G.; Wu, J.; Gu, B. L.; Duan, W. *Appl. Phys. Lett.* **2006**, *89*, 1731301.
(22) Suzuki, S.; Watanabe, Y.; Kiyokura, T.; Nath, K. G.; Ogino, T.; Heun, S.; Zhu, W.; Bower, C.; Zhou, O. *Phys. Rev. B* **2001**, *63*, 245418.
(23) Speranza, G.; Minati, L. *J. Phys. Chem. C* **2008**, *112*, 14412.
(24) Pichler, T.; Knupfer, M.; Golden, M. S.; Fink, J.; Rinzler, A.; Smalley, R. E. *Phys. Rev. Lett.* **1998**, *80*, 4729.
(25) Abiman, P.; Crossley, A.; Wildgoose, G. G.; Jones, J. H.; Compton, R. G. *Langmuir* **2007**, *23*, 7847.
(26) Tanaka, K.; Miura, T.; Umezawa, N.; Urano, Y.; Kikuchi, K.; Higuchi, T.; Nagano, T. *J. Am. Chem. Soc.* **2001**, *123*, 2530.
(27) Zhao, Q. L.; Zhang, Z. L.; Huang, B. H.; Peng, J.; Zhang, M.; Pang, D. W. *Chem. Commun.* **2008**, *41*, 5116.
(28) Liu, H.; Ye, T.; Mao, C. *Angew. Chem., Int. Ed.* **2007**, *46*, 6473.
(29) Pan, D.; Zhang, J.; Li, Z.; Wu, M. *Adv. Mater.* **2009**, *21*, 1.

JP101868S